Coexistence of Crumpling and Flat Sheet Conformations in Two-Dimensional Polymer Networks: An Understanding of Aggrecan Self-Assembly

Alexandros Chremos[*,†] and Ferenc Horkay
Section on Quantitative Imaging and Tissue Sciences,
Eunice Kennedy Shriver National Institute of Child Health and Human Development,
National Institutes of Health, Bethesda, Maryland 20892, USA

(Received 11 January 2023; revised 12 July 2023; accepted 8 September 2023; published 28 September 2023)

We investigate the conformational properties of self-avoiding two-dimensional (2D) ideal polymer networks with tunable mesh sizes as a model of self-assembled structures formed by aggrecan. Polymer networks having few branching points and large enough mesh tend to crumple, resulting in a fractal dimension of $d_f \approx 2.7$. The flat sheet behavior ($d_f = 2$) emerges in 2D polymer networks having more branching points at large length scales; however, it coexists with crumpling conformations at intermediate length scales, a feature found in scattering profiles of aggrecan solutions. Our findings bridge the long-standing gap between theories and simulations of polymer sheets.

DOI: 10.1103/PhysRevLett.131.138101

Sheetlike two-dimensional (2D) polymers have attracted considerable attention in manufacturing and electronics applications as composites associated with energy storage [1,2] and 3D printing [3,4]. Graphene is perhaps the most familiar realization of this type of polymeric structure [5,6]. They are also prevalent structures in biology in the form of open membranelike structures or closed vesicular structures that exhibit biological functions in living systems. Well-known examples include living cell membranes [7,8] and red blood cell cytoskeletons [9,10]. Recently, there have been efforts to create such structures synthetically, such as DNA origami [11–13] and as vehicles for precision medicine [14]. Finally, as in the case of linear polymer chains, these structures arise as natural mathematical objects in the high-energy physics and field theory [15].

Unlike linear chain polymers, 2D polymers exhibit exotic conformational properties since no single universality class encompasses all types of surfaces [16]. Theoretical models [8,17] initially suggested that 2D polymers in good solvent exhibit a flat conformation, corresponding to a Flory exponent of $\nu = 1/2$ [18], but beyond a characteristic size it was predicted that they should "crumple" due to thermal fluctuations, in a fashion similar to linear polymers having a length larger than their "persistence length" [19]. The Flory-type approximation for ν of these hypothetical crumpled sheets was $\nu = 0.4$ [20,21], while subsequent independent theoretical arguments predicted an exponent in the range $\nu \approx 0.35 \pm 0.07$ [8,22–24]. An exponent $\nu < 1/2$ has been observed experimentally in partially polymerized vesicles [25–27] and in graphite oxide membranes [28,29] suggesting the possibility of the predicted crumpling transition. However, extensive computer simulations convincingly demonstrated that in the presence of excluded volume interactions, 2D polymers stabilize the flat sheet conformation in a good solvent and thus do not crumple [10,30–34]. The nature and even the existence of a crumpling transition remains unresolved.

The gap between the theory and simulations is attributed to the nontrivial influence of excluded volume, which is a local effect and intrinsic in molecular models, on the shape of the whole structure. However, this influence is absent in the theoretical framework just mentioned [10,34]. We note that previously used molecular models of 2D polymers have a small or no mesh size. This structural feature was thought to be essential to mimic the continuous description of 2D polymers used in theories, and its influence has remained unexplored. To bridge this gap, we hypothesize that by increasing the mesh size, the excluded volume interactions progressively become weaker since the probability of segment-segment contacts is expected to decrease while the network's topology is maintained. Effectively, the mesh size provides a way to reduce the influence of excluded volume; a similar conclusion was reached in perforated 2D sheets [35]. Our proposed 2D polymer network model also draws inspiration from recent advancements in the synthesis of precisely controlled polymer networks that bring us closer to the realization of ideal 2D polymer networks [36–39].

Our study's original and unexpected motivation is to understand the nature of self-assembled structures formed by aggrecan, a bottlebrush-like polymer and an essential component in the extracellular matrices of living systems. In articular cartilage, aggrecan associates with hyaluronic acid and a small glycoprotein, a link protein, to form hierarchical polymeric networks within an extracellular organized fibrillar collagen network [40,41]. These networks exert a high osmotic swelling pressure necessary for cartilage to resist external compressing loads. Moreover,

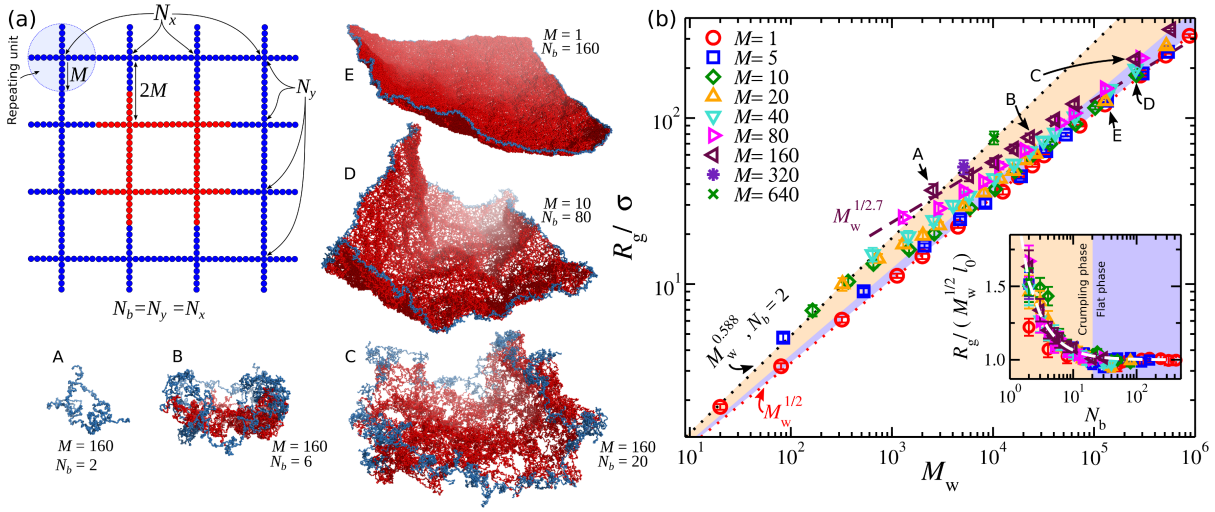

FIG. 1. (a) Schematic of a regular 2D polymer network having $N_b = 4$ branches in each direction. Screenshots of typical equilibrated 2D polymer networks are also presented. For clarity, the repeating units located at the edge of the polymer network are in blue and for the units in the middle in red. (b) Radius of gyration R_g of 2D polymer networks as a function of molecular mass M_w. The highlighted regimes approximately outline the emergence of crumpling (pale yellow) and flat sheet regimes (pale blue). The dotted lines are power laws with an exponent of 0.588 and 1/2 and the dashed line is a power law with an exponent of 1/2.7; all lines are guides for the eye. The uncertainty estimates correspond to two standard deviations. Inset: R_g normalized by $M_w^{1/2}$ and l_0 as a function of N_b. The dashed line is $R_g \approx l_0 M_w^{1/2}(1.3/N_b^{1.3} + 1)$.

the structure of aggrecan assemblies exhibits ion insensitivity, and it is opposite to the typical behavior of polyelectrolyte solutions, which phase separate in the presence of high valence ions [42,43]. This ion insensitivity is essential in aggrecan participation in cartilage skeletal metabolism contributing to bone mineralization by binding calcium ions [44,45]. Despite extensive experimental studies on the structure of aggrecan assemblies [44–47], a microscopic model to reproduce the observed behavior is missing. In particular, we have investigated recently the structures of aggrecan solutions and compared them to structures of synthetic bottlebrush polymers in which the chemical composition of the backbone and the side chains were carefully controlled [48,49]. These studies revealed that typical molecular models found in the literature provide a good agreement with the synthetic (neutral or charged) bottlebrushes but fail to describe the polymer network structures formed by aggrecan, suggesting nontrivial aggrecan association interactions. We then felt that a molecular model of aggrecan assemblies was required to understand this important class of biological materials.

We briefly describe the simulation model; additional details on the simulations and experimental methodologies can be found in the Supplemental Material (SM) [50]. We use molecular dynamics simulation of a bead-spring model suspended in an implicit solvent, previously used in the modeling of gels and nanogel particles [56,57]. All particles are assigned the same mass m, size σ, and strength of interaction ε; we set ε and σ as the units of energy and length. The segmental interactions are described by the cut-and-shifted Lennard-Jones (LJ) potential with a cutoff distance corresponding to an athermal solvent. The segments along a chain are connected with their neighbors via a stiff harmonic spring to avoid bond crossing. The 2D polymer network is composed of repeating units arranged in a square lattice and with two or more of the free ends connected with the neighboring repeating units, see Fig. 1(a). A repeating unit has a core particle connected to one of the free ends of $f = 4$ chains, and each chain is composed of M segments. The number of repeating units in each direction is labeled as N_x and N_y. We focus on symmetric 2D sheets having $N_b = N_x = N_y$. The molecular mass of a 2D polymer network is $M_w = N_b^2(fM + 1)$. Previous coarse-grained models [30–34] of 2D polymers correspond in our model as the limiting case of $M = 0$.

The mass scaling of the radius of gyration (R_g) of equilibrated 2D polymer networks in good solvent conditions exhibits a nontrivial behavior. We identify two limiting behaviors. On the one hand, 2D polymer networks having $N_b = 2$, where the influence of branching is minimum, exhibit a mass scaling $R_g \sim M_w^{\nu}$ with $\nu = 0.588$. An exponent similar to the mass scaling exponent for self-avoiding random walks suggests that the structure is dominated by the linear chain statistics in an athermal solvent, see Fig. 1(b). On the other hand, a mass scaling of $R_g \sim M_w^{1/2}$ is found for 2D polymer networks having small mesh size $1 \leq M \lesssim 4$ for the range of N_b values explored here and the molecular conformations resemble a flat sheet, Fig. 1. A similar scaling behavior $R_g \sim M_w^{1/2}$ is found for

2D polymer networks having $N_b > 20$ irrespective of the value of M. Specifically, we find that the mesh size influences the prefactor in this mass scaling behavior, $R_g \approx l_0 M_w^{1/2}$, where l_0 is found to have a weak dependence on M as follows: $l_0 \approx M^{0.08}/3.28$. This $\nu = 1/2$ exponent is also the exact solution proposed by Parisi for randomly branched polymers [58]. These results would seem to indicate that randomly branched polymers can be viewed as perforated polymer sheets [56,59,60]. The same scaling exponent also appears in scattering profiles at large length scales, which we will discuss below, in complex materials such as gels [61,62], polyelectrolyte complexation [63], colloidal aggregates [64], and random porous materials [65].

Between the flat sheet behavior and the regime dominated by linear chain behavior, we find a crossover regime where the molecular parameter space (M, N_b) of the above-mentioned limiting behaviors describes 2D polymer networks when the mesh size (characterized by M) becomes comparable to the polymer network's size $N_b < 20$ and $M \gg 1$. The mass scaling exponent in this crossover regime is found to be $\nu \approx 1/2.7 \approx 0.37$ for fixed M, see Fig. 1(b). This effect is more pronounced for larger mesh sizes. A smaller value of ν means that the molecular conformations deviate from the flat sheet conformation and resemble crumpled sheets; compare screenshots in Fig. 1(a). All the 2D polymer network R_g data can overlap, suggesting a universal behavior, according to the following zero-order approximation: $R_g \approx l_0 M_w^{1/2}(1.3/N_b^{1.3} + 1)$, see inset Fig. 1(b). The flat sheet state occurs when the 2D polymer network is large enough, i.e., $1.3/N_b^{1.3} \approx 0$.

To quantify the spatial correlations between the polymer segments in the 2D polymer networks, we calculate the polymer networks' form factor $P(q)$. The scattering profile exhibits two common structural features found in the calculation of $P(q)$ of polymeric materials: a peak at $q\sigma \approx 7$ corresponding to the distance between the bonded segments and $P(q)$ reaches a plateau $P(q) \approx M_w$ in the low q regime, known as the Guinier region. Based on previous understanding of polymer sheets, at intermediate length scales, the form factor $P(q)$ is expected to be described by a single power law, i.e., $P(q) \sim q^{-2}$. However, a deviation emerges at shorter length scales as the mesh size increases in the 2D polymer networks in the flat sheet states (based on the R_g scaling), see Fig. 2 reveals a deviation at shorter length scales, see Fig. 2. The 2D polymer networks exhibit a hierarchical and complex structure described by three power-law regimes, $P(q) \sim q^{-1/\nu}$, where the scaling exponent ν describes the nature of polymer segment correlations in each of the associated regimes, see Fig. 3(a). These regimes are the linear chain, the mesh, and the flat sheet. Moreover, $P(q)$ curves of 2D polymer networks, having the same M, overlap before reaching the Guinier region.

The linear chain regime is associated with relatively small length scales where a single polymer chain within the polymer network structure is probed, i.e., smaller than the mesh size. In this regime, the scattering profile $P(q)$ scales with an exponent $-1/\nu \approx -1.7$ corresponding to $\nu \approx 0.588$, see Fig. 3. Polymer networks dominated by this power-law regime have $N_b = 2$ and they exhibit $R_g \sim M_w^{0.588}$ as seen in Fig. 1(b). Larger length scales than the linear chain regime, corresponding to polymer networks having $N_b > 2$, are associated with the emergence of the mesh structure (partial structure of the network). In these length scales, we observe an extensive power-law regime with an apparent power law of $\nu \approx 0.37$, corresponding to a "fractal" dimension $1/\nu = d_f = 2.7$. This is the expected value of d_f for branched polymers having a relatively high grafting density or a three-dimensional network corresponding to the θ value of the Wiener sheet model [60]. At this regime, the 2D polymer networks resemble crumpling sheets and R_g scales as $R_g \sim M_w^{1/2.7}$, see Fig. 1(b). The range of this power-law regime increases by increasing N_b until $N_b \approx 20$. This -2.7 exponent is not influenced by changing the topology of the mesh in the polymer network; an example of a triangular lattice is presented in the SM [50]. A similar crossover has also been noted recently for the scattering patterns of the aggregates of carbon nanotubes in solution [66]. For polymer sheets having $N_b > 20$ and at lower q values $q \lesssim 2\pi/R_g$, where a significant part of the network structure is probed, we find the emergence of the third power-law regime associated with d_f expected for polymer sheets, $d_f = 2$. In other words, the flat sheet characteristics emerge in $P(q)$ once $N_b > 20$ irrespective of the mesh size, see Fig. 3. This is consistent with the emergence of power-law exponent $\nu = 1/2$ in the mass scaling of R_g, as discussed above. The location of the

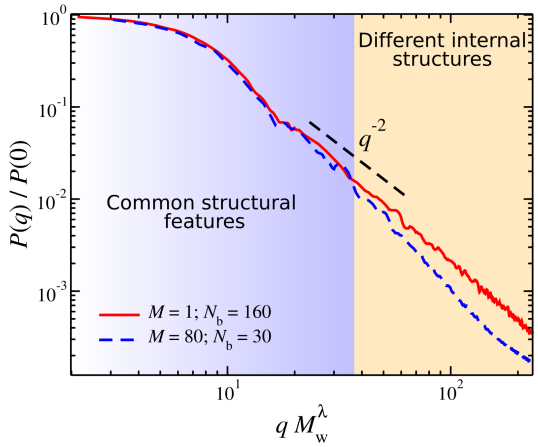

FIG. 2. Form factor $P(q)$ of polymer networks having two different mesh sizes. The highlighted regimes approximately outline the regions at which the polymer networks exhibit common structural features and where they deviate due to differences in the internal structure of these polymer networks. The exponent λ is a parameter to overlap the normalized $P(q)$ curves in the low q regime.

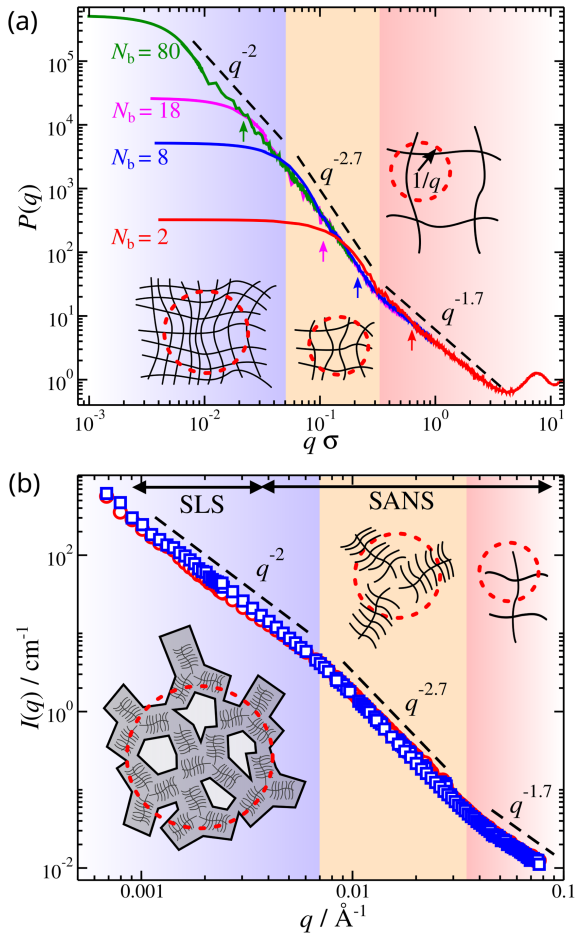

FIG. 3. (a) Form factor $P(q)$ of polymer networks having chain length $M = 20$ based on our simulation model. The highlighted regimes approximately outline the different power-law regimes that the polymer networks exhibit. The dashed lines indicate power laws as guides to the eye. The drawings illustrate structural features probed at different length scales in 2D polymer networks. The vertical arrows approximately point to the size of the corresponding polymer network, $q\sigma = 2\pi/R_g$. (b) Combined static light scattering (SLS) and small angle neutron scattering (SANS) measurements of the scattering from 0.1% (w/w) aggrecan solutions with no salt (circles) and 100 mM $CaCl_2$ (squares). The drawings illustrate aggrecan assemblies probed at different length scales; an outline of the self-assembled structures is drawn for the case of low q to highlight the 2D polymer network formation. The experimental data are from Refs. [44,45].

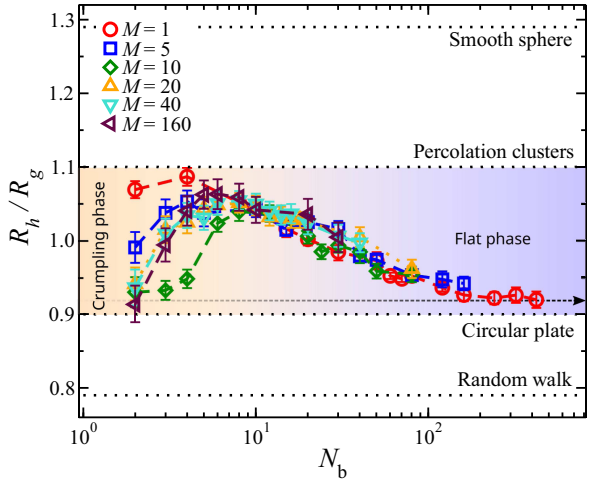

FIG. 4. Ratio of the hydrodynamic radius over the radius of gyration R_h/R_g as a function of the number of branched points in each direction of the 2D polymer network N_b. From top to bottom, the dotted lines correspond to the exact results of R_h/R_g for uniform spheres, circular discs, and an estimate of the ratio for random walks and percolation clusters [69]. The dashed arrow points to the plateau reached by large molecular mass polymer sheets $R_h/R_g \approx 0.92$. The uncertainty estimates correspond to one standard deviation.

crossover from one power-law regime to another (from linear chain to mesh and from the mesh to flat sheet regimes) of 2D polymer networks having $N_b > 20$ scale as $q \sim M^{-3/5}$; see SM [50] for more details.

Aggrecan association results in the formation of clusters whose structure resembles that of the crumpling structures found in our model; see SM [50] for details of the experimental setup. Figure 3(b) shows the combined neutron (SANS) and SLS spectra of aggrecan solutions. The absence of a plateau regime at low q shows that the size of these clusters exceeds the resolution of the light scattering measurements, i.e., several hundred nanometers. The structure of the aggrecan assemblies is poorly defined, but our model provides key insights. The mesh structure in our 2D polymer network model appears to be an essential characteristic of aggrecan solutions. We note that breaking the bonds between repeating units without deteriorating the 2D polymer network structure up to the percolation threshold results in the disappearance of the mesh regime in $P(q)$ [56], suggesting aggrecan assemblies have a mesh with closed-loop structures. Moreover, only 2D polymer networks with no or few defects exhibit the -2.7 scaling at intermediate length scales at scattering profiles. Randomly branched structures where the connectivity is isotropic have their excluded volume interactions screened, resulting in the absence of this structural feature [56,67]. Thus, our findings suggest that aggrecan self-associates to form structures with closed loops resembling flat sheets at longer length scales. The full scattering profile of aggrecan solutions exhibits an additional rodlike behavior at length scales of a few monomers related to the stiff side chains; see the SM [50] on how our model captures this behavior.

We return to characterizing the crumpling state. We calculate the hydrodynamic radius (R_h) with ZENO package [68] and utilize the ratio R_h/R_g to quantify the shape of the 2D polymer networks; see SM [50] for more details. The values of R_h/R_g for a smooth sphere is 1.29, for a random walk is 0.79, and for an infinitely long rod is 0 [69,70]. There is a peak in $R_h/R_g \approx 1.05$ (close to percolation clusters [69]) at $N_b \approx 7$, indicating the highest degree of crumpling sheet conformations, see Fig. 4. The 2D polymer

networks at this peak tend to *curl*, evident from negative values of normal-normal correlations at large distances presented in the SM [50]. As N_b increases, normal-normal correlations decay more slowly, indicating the emergence of resistance to curling and bending; see the SM [50]. Moreover, R_h/R_g decreases until it reaches a plateau at $R_h/R_g \approx 0.92$ for $N_b \gtrsim 200$, corresponding to the flat sheet conformation, which is slightly larger than the molecular shape of circular plates, $R_h/R_g \approx 0.9$ [69]. The difference is due to the fluctuations in the polymer network, effectively making the sheet's thickness thicker than a nonfluctuating circular plate.

We utilized a coarse-grained self-avoiding two-dimensional polymer network model having a tunable mesh size to bridge the gap between the theory and simulation models on polymer sheets and to gain insights about the nature of aggrecan assemblies in solution. Increasing the mesh size in our model, which was not found previously in molecular sheet models, reduces the strength of the effective excluded volume interactions, resulting in the emergence of crumpling conformations. The crumpling conformations have a fractal dimension of $d_f = 2.7$, a somewhat larger value than predicted by the Flory theory for crumpled 2D polymers. This state occurs once the mesh size becomes comparable to the size of the overall polymer network. However, irrespective of the mesh size, we find a fractal dimension of $d_f = 2$, resembling flat sheets, for 2D polymer networks having more branching points $N_b > 20$. In other words, crumpling emerges in small polymer networks, i.e., having few branching points, contrary to the theoretical predictions that crumpling would emerge in large polymer sheets beyond a characteristic length scale. The scattering profiles of the larger 2D polymer networks exhibit complex structural features, where both flat and crumpling features coexist at different length scales, indicating an alternative foundation to the previous understanding of having flat and crumpling as exclusive states. This coexistence of structural features is found in the structure of aggrecan solutions, thus providing a framework for developing bottlebrush models that can reproduce the observed associative behavior of aggrecan.

The authors thank J. F. Douglas for insightful discussions. This research was supported by the Intramural Research Program of the *Eunice Kennedy Shriver* National Institute of Child Health and Human Development, NIH. We acknowledge the support of the National Institute of Standards and Technology, U.S. Department of Commerce, in providing the neutron research facilities used in this work.

*alexandros.chremos@nih.gov
†Present address: Chemical Sciences Division, National Institute of Standards and Technology, Gaithersburg, Maryland 20899–8320, USA.

[1] S. Stankovich, D. A. Dikin, G. H. Dommett, K. M. Kohlhaas, E. J. Zimney, E. A. Stach, R. D. Piner, S. T. Nguyen, and R. S. Ruoff, Nature (London) **442**, 282 (2006).
[2] P. Xiao and Y. Xu, J. Mater. Chem. A **6**, 21676 (2008).
[3] Z. Liang, Y. Pei, C. Chen, B. Jiang, Y. Yao, H. Xie, M. Jiao, G. Chen, T. Li, B. Yang *et al.*, ACS Nano **13**, 12653 (2019).
[4] S. Melo, S. C. Neves, A. T. Pereira, I. Borges, P. L. Granja, F. D. Magalhães, and I. C. Gonçalves, Mater. Sci. Eng. C **109**, 110537 (2020).
[5] A. K. Geim and K. S. Novoselov, Nat. Mater. **6**, 183 (2007).
[6] J. C. Meyer, A. K. Geim, M. I. Katsnelson, K. S. Novoselov, T. J. Booth, and S. Roth, Nature (London) **446**, 60 (2007).
[7] R. Lipowsky, Nature (London) **349**, 475 (1991).
[8] M. J. Bowick and A. Travesset, Phys. Rep. **344**, 255 (2001).
[9] C. F. Schmidt, K. Svoboda, N. Lei, I. B. Petsche, L. E. Berman, C. R. Safinya, and G. S. Grest, Science **259**, 952 (1993).
[10] G. S. Grest and I. B. Petsche, Phys. Rev. E **50**, R1737 (1994).
[11] S. Perrier, Nat. Chem. **3**, 194 (2011).
[12] A. Kuzuya and Y. Ohya, Acc. Chem. Res. **47**, 1742 (2014).
[13] P. Y. Chen, M. Liu, Z. Wang, R. H. Hurt, and I. Y. Wong, Adv. Mater. **29**, 1605096 (2017).
[14] S. Y. Wu, S. S. A. An, and J. Hulme, Int. J. Nanomed. **10**, 9 (2015).
[15] K. G. Wilson, Phys. Rev. D **10**, 2445 (1974).
[16] M. E. Cates, Phys. Lett. B **161**, 363 (1985).
[17] G. Gompper and D. M. Kroll, J. Phys. Condens. Matter **9**, 8795 (1997).
[18] U. Glaus, Phys. Rev. Lett. **56**, 1996 (1986).
[19] C. Jeong and J. F. Douglas, J. Chem. Phys. **143**, 144905 (2015).
[20] Y. Kantor, M. Kardar, and D. R. Nelson, Phys. Rev. Lett. **57**, 791 (1986).
[21] Y. Kantor and D. R. Nelson, Phys. Rev. A **36**, 4020 (1987).
[22] F. David and E. Guitter, Europhys. Lett. **5**, 709 (1988).
[23] P. Le Doussal and L. Radzihovsky, Phys. Rev. Lett. **69**, 1209 (1992).
[24] D. Espriu and A. Travesset, Nucl. Phys. **B468**, 514 (1996).
[25] M. Mutz, D. Bensimon, and M. J. Brienne, Phys. Rev. Lett. **67**, 923 (1991).
[26] M. S. Spector, E. Naranjo, S. Chiruvolu, and J. A. Zasadzinski, Phys. Rev. Lett. **73**, 2867 (1994).
[27] S. Chaieb, V. K. Natrajan, and A. A. El-rahman, Phys. Rev. Lett. **96**, 078101 (2006).
[28] X. Wen, C. W. Garland, T. Hwa, M. Kardar, E. Kokufuta, Y. Li, M. Orkisz, and T. Tanaka, Nature (London) **355**, 426 (1992).
[29] W. M. El Rouby, RSC Adv. **5**, 66767 (2015).
[30] M. Plischke and D. Boal, Phys. Rev. A **38**, 4943 (1988).
[31] F. F. Abraham, W. E. Rudge, and M. Plischke, Phys. Rev. Lett. **62**, 1757 (1989).
[32] S. Leibler and A. C. Maggs, Phys. Rev. Lett. **63**, 406 (1989).
[33] F. F. Abraham and D. R. Nelson, Science **249**, 393 (1990).
[34] Y. Kantor and K. Kremer, Phys. Rev. E **48**, 2490 (1993).
[35] D. Yllanes, S. S. Bhabesh, D. R. Nelson, and M. J. Bowick, Nat. Commun. **8**, 1381 (2017).
[36] D. F. Perepichka and F. Rosei, Science **323**, 216 (2009).
[37] J. W. Colson and W. R. Dichtel, Nat. Chem. **5**, 453 (2013).

[38] K. Baek, G. Yun, Y. Kim, D. Kim, R. Hota, I. Hwang, D. Xu, Y. H. Ko, G. Gu, J. H. Suh *et al.*, J. Am. Chem. Soc. **135**, 6523 (2013).
[39] S. Nakagawa and N. Yoshie, Polym. Prepr. **13**, 2074 (2022).
[40] J. A. Buckwalter and H. J. Mankin, J. Bone Joint Surg. **79**, 600 (1997), https://journals.lww.com/jbjsjournal/citation/1997/04000/instructional_course_lectures,_the_american.21.aspx.
[41] J. A. Buckwalter and H. Mankin, J. Bone Joint Surg. **79**, 612 (1997), https://journals.lww.com/jbjsjournal/citation/1997/04000/instructional_course_lectures,_the_american.22.aspx.
[42] M. Muthukumar, Macromolecules **50**, 9528 (2017).
[43] B. Zheng, Y. Avni, D. Andelman, and R. Podgornik, J. Phys. Chem. **125**, 7863 (2021).
[44] F. Horkay, P. J. Basser, A. M. Hecht, and E. Geissler, J. Chem. Phys. **128**, 135103 (2008).
[45] F. Horkay, P. J. Basser, A. M. Hecht, and E. Geissler, Phys. Rev. Lett. **101**, 068301 (2008).
[46] F. Horkay, P. J. Basser, A. M. Hecht, and E. Geissler, Macromol. Symp. **306**, 11 (2011).
[47] F. Horkay, P. J. Basser, A. M. Hecht, and E. Geissler, Macromol. Symp. **372**, 43 (2017).
[48] F. Horkay, A. Chremos, J. F. Douglas, R. Jones, J. Lou, and Y. Xia, J. Chem. Phys. **152**, 194904 (2020).
[49] F. Horkay, A. Chremos, J. F. Douglas, R. Jones, J. Lou, and Y. Xia, J. Chem. Phys. **155**, 074901 (2021).
[50] See Supplemental Material at http://link.aps.org/supplemental/10.1103/PhysRevLett.131.138101, which includes Refs. [51–55], for additional details on the model and methods, as well as additional results.
[51] J. B. Hubbard and J. F. Douglas, Phys. Rev. E **47**, R2983 (1993).
[52] M. L. Mansfield, J. F. Douglas, and E. J. Garboczi, Phys. Rev. E **64**, 061401 (2001).
[53] M. L. Mansfield, A. Tsortos, and J. F. Douglas, J. Chem. Phys. **143**, 124903 (2015).
[54] E. H. Kang, M. L. Mansfield, and J. F. Douglas, Phys. Rev. E **69**, 031918 (2004).
[55] J. F. Douglas and E. J. Garboczi, Adv. Chem. Phys. **91**, 85 (1995).
[56] A. Chremos, F. Horkay, and J. F. Douglas, J. Chem. Phys. **156**, 094903 (2022).
[57] A. Chremos, J. F. Douglas, P. J. Basser, and F. Horkay, Gels **8**, 707 (2022).
[58] G. Parisi and N. Sourlas, Phys. Rev. Lett. **46**, 871 (1981).
[59] G. S. Grest and M. Murat, J. Phys. **51**, 1415 (1990).
[60] J. F. Douglas, Phys. Rev. E **54**, 2677 (1996).
[61] S. Seiffert, Prog. Polym. Sci. **66**, 1 (2017).
[62] M. Shibayama, X. Li, and T. Sakai, Colloid Polym. Sci. **297**, 1 (2019).
[63] E. Spruijt, F. A. Leermakers, R. Fokkink, R. Schweins, A. A. van Well, M. A. Cohen Stuart, and J. van der Gucht, Macromolecules **46**, 4596 (2013).
[64] D. W. Schaefer, J. E. Martin, P. Wiltzius, and D. S. Cannell, Phys. Rev. Lett. **52**, 2371 (1984).
[65] D. W. Schaefer and K. D. Keefer, Phys. Rev. Lett. **56**, 2199 (1986).
[66] B. J. Bauer, E. K. Hobbie, and M. L. Becker, Macromolecules **39**, 2637 (2006).
[67] A. Chremos, F. Horkay, and J. F. Douglas, J. Chem. Phys. **155**, 134905 (2021).
[68] D. Juba, D. J. Audus, M. Mascagni, J. F. Douglas, and W. Keyrouz, J. Res. Natl. Inst. Stand. Technol. **122**, 20 (2017).
[69] M. L. Mansfield and J. F. Douglas, J. Chem. Phys. **139**, 044901 (2013).
[70] M. L. Mansfield and J. F. Douglas, Macromolecules **41**, 5422 (2008).